Marginal Fermi Liquid in a lattice of three-body bound-states.

A. F. Ho[1,2] and P. Coleman[1,2]
[1]*Serin Laboratory, Rutgers University, P.O. Box 849, Piscataway, New Jersey 08855-0849*
[2]*Department of Physics, University of Oxford, 1 Keble Road, Oxford OX1 3NP, UK*

We study a lattice model for Marginal Fermi liquid behavior, involving a gas of electrons coupled to a dense lattice of three-body bound-states. The presence of the bound-states changes the phase space for electron-electron scattering and induces a marginal self-energy amongst the electron gas. When the three-body bound-states are weakly coupled to the electron gas, there is a substantial window for marginal Fermi liquid behavior and in this regime, the model displays the presence of two relaxation times, one linear, one quadratic in the temperature. At low temperatures the bound-states develop coherence leading to a cross-over to conventional Fermi liquid behavior. At strong-coupling, marginal Fermi liquid behavior is pre-empted by a pairing or magnetic instability, and it is not possible to produce a linear scattering rate comparable with the temperature. We discuss the low temperature instabilities of this model and compare it to the Hubbard model at half-filling.

72.15.Nj, 71.30+h, 71.45.-d

I. INTRODUCTION

The concept of a marginal Fermi liquid (MFL) was invented as a phenomenological description of the asymptotic properties of of high temperature superconductors in their normal state[1]. These include a linear electrical resistivity $\rho \sim T$ over at least 2 decades in temperature and a quasi-particle scattering rate which may be proportional to frequency up to energies as high as 750 meV.[2,3] Even in underdoped cuprate superconductors, optical data indicates that marginal behavior develops at scales above the spin gap.[4] We shall take a marginal Fermi liquid to be a system of fermions with an inelastic scattering rate of the form

$$\Gamma \propto \max[|\ \omega\ |, T], \tag{1}$$

where there is no significant momentum dependence of Γ. In the cuprates, the constant of proportionality is of order unity. Analyticity then ensures that the appropriate self-energy takes the form

$$\Sigma(\omega) \sim \omega \ln \max[|\ \omega\ |, T]. \tag{2}$$

Many proposals have been made to explain the origin of this unusual behavior. One prevalent idea, is that the marginal Fermi liquid behavior derives from scattering off a soft bosonic mode. This idea underpins the Van Hove scenario[5], gauge theory models[6] and the quantum-critical scattering[7] picture of the cuprates. By contrast, Anderson[8] proposes that the cuprate metal is a fully developed Luttinger liquid, with power-law self-energies which have been mis-identified as a logarithm. Since the soft-mode theories furnish an electron self-energy which is strongly momentum dependent, none of these proposals actually gives rise to a marginal Fermi liquid as originally envisaged.

In this paper, we return to the original proposal, asking whether a marginal Fermi liquid can form in a dense electronic system. We pursue an early speculation, due to Ruckenstein and Varma[9], that the marginal self-energy might derive from the scattering of conduction electrons off a dispersionless localized bound-state Φ at the Fermi energy, giving rise to the interaction:

$$H_{int} = \lambda(c^+_{i\uparrow} c_{i\uparrow} c^+_{i\downarrow} \Phi + h.c.). \tag{3}$$

The presence of such states precisely at the Fermi surface would mean that the three-particle phase space grows linearly with energy. Inelastic scattering into the localized bound-state then leads to a marginal self-energy in leading order perturbation theory, as illustrated in Fig. 1. (The localised state is represented by the dash line.) Since the hypothetical object at the Fermi surface scatters electrons in triplets, Ruckenstein and Varma identified it as a three-body bound state.

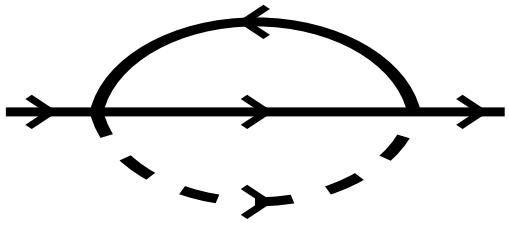

FIG. 1. Marginal self-energy diagram for the band electrons. Notation: thick lines denote band electron propagators, dashed lines denote the localised state propagator.

A great difficulty with this picture is that it cannot be made self-consistent. At the same level of perturbation

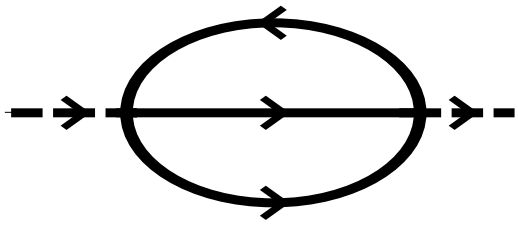

FIG. 2. Self-energy for the localised state.

theory that furnishes a marginal self-energy, the three-body state must scatter off the electrons to produce a self-energy term of the form shown in Fig 2. This self-energy correction inevitably moves the resonance of the three-body bound-state away from the Fermi energy, introducing an unwanted scale into the problem and causing the singular scattering to disappear.

An unexpected resolution of this problem recently appeared in the context of the single impurity two-channel Kondo model[10]. Marginal Fermi liquid behavior does develop in this model, and the mechanism by which it occurs is remarkably close to the original three-body bound-state proposal, with one critical difference: in the two-channel Kondo model, the three-body bound-state formed at the impurity site carries no internal quantum numbers (spin and charge). The associated bound-state fermion is represented by a Hermitian operator:

$$\Phi = \Phi^\dagger. \tag{4}$$

This type of fermion is known as a Majorana fermion[14] *. The effective action for such a field must have the form:

$$S = \int d\omega \Phi(-\omega)(\omega - \Sigma(\omega))\Phi(\omega). \tag{5}$$

Since $\Phi(-\omega)\Phi(\omega) = -\Phi(\omega)\Phi(-\omega)$ due to the Grassmanian nature of Φ, $\Sigma(\omega)$ will be an odd function of frequency, so that $\Sigma(0) = 0$. In other words, the particle-hole symmetry of the Φ field guarantees that its energy is pinned to the Fermi surface.

In the two-channel Kondo model (after dropping the charge degrees of freedom, thanks to spin-charge decoupling[16]), the total spin $\vec{S}$ of the two conduction channels at the impurity site can be written in the form: $\vec{S} = -\frac{i}{2}\vec{\Psi}(0) \times \vec{\Psi}(0)$ where $\vec{\Psi} = (\Psi^{(1)}, \Psi^{(2)}, \Psi^{(3)})$ is a triplet of Majorana fermions. These three high energy degrees of freedom bind at the impurity site to form the localised three-body bound-state $\Phi(0)$, represented as the contraction of the three fermions:

$$\Psi^{(1)}(0)\Psi^{(2)}(0)\Psi^{(3)}(0) = A\Phi(0), \tag{6}$$

where A is the amplitude for forming this pole Φ. The residual interaction with the bulk spin degrees of freedom in the low energy world then gives rise to a vertex of the form $\lambda\Psi^{(1)}\Psi^{(2)}\Psi^{(3)}\Phi$. The challenge here is to see if such a mechanism could be generalised to a more realistic lattice model. The work described below is an attempt to make a first step in this direction.

II. CONSTRUCTION OF MODEL

We now use these ideas to motivate a simple *lattice* model of a marginal Fermi Liquid. First note that the Hubbard model at half-filling can be rewritten in a Majorana fermion representation[11], by the following two steps. The Hubbard model is:

$$H_{Hubbard} = t\sum_{i,a,\sigma}(c^\dagger_{i+a,\sigma}c_{i,\sigma} + H.c.) + U\sum_i (c^\dagger_{i\uparrow}c_{i\uparrow} - 1/2)(c^\dagger_{i\downarrow}c_{i\downarrow} - 1/2). \tag{7}$$

In the first step, we assume that the lattice has a bipartite structure, and do a gauge transformation on electron operators belonging to one sublattice of the bipartite lattice: $c_{i\sigma} \to -ic_{i\sigma}$. Also let the hopping term connect a sublattice A site only to a sublattice B site, and not to other sublattice A sites. Then the interaction is unchanged, but the kinetic energy becomes:

$$H_{K.E.} = it\sum_{i,a,\sigma}(c^\dagger_{i+a,\sigma}c_{i,\sigma} + H.c.). \tag{8}$$

Next, rewrite the electron operators using $c_\uparrow = \frac{1}{\sqrt{2}}(\Psi^{(1)} - i\Psi^{(2)}), c_{i\downarrow} = -\frac{1}{\sqrt{2}}(\Psi^{(3)} + i\Psi^{(0)})$ where the $\Psi^{(a)}$'s are Majorana fermions, and we get:

$$H_{Hubbard} = it\sum_{i,c}\sum_{a=0}^{3}\Psi^{(a)}_{i+c}\Psi^{(a)}_i - U\sum_i \Psi^{(0)}_i\Psi^{(1)}_i\Psi^{(2)}_i\Psi^{(3)}_i. \tag{9}$$

(Note the sign change for the interaction.) In Majorana representation, we see explicitly the $SO(4)$ symmetry[1112] of the Hubbard model at half-filling.

The crucial generalisation of this paper is to break the $SO(4)$ symmetry down to $O(3)$, setting:

$$t \to t_a = \begin{cases} t & : \quad a = 1,2,3 \\ t_0 & : \quad a = 0. \end{cases}. \tag{10}$$

With $\Phi_i \equiv \Psi^{(0)}_i$,

$$H = it_0\sum_{i,c}\Phi_{i+c}\Phi_i + it\sum_{i,c}\sum_{a=1}^{3}\Psi^{(a)}_{i+c}\Psi^{(a)}_i - U\sum_i \Phi^{(0)}_i\Psi^{(1)}_i\Psi^{(2)}_i\Psi^{(3)}_i. \tag{11}$$

*Such an object can always be constructed as a linear combination of two charged fermions $\Phi = \frac{1}{\sqrt{2}}(a + a^\dagger)$.

When $t_0 = 0$, this Hamiltonian describes a lattice of localised three-body bound-states Φ_i coupled to the continuum.

This toy model provides a simple system to study the properties of these pre-formed bound-states at each site. A microscopic model would provide an explanation of the origin of this symmetry breaking field leading to formation of these bound-states. In this work, we do not address this issue, but instead, ask whether the single impurity marginal Fermi Liquid mechanism survives in the lattice, in this model of reduced symmetry.

We shall show that the main physical effect of the lattice (in the absence of a broken symmetry phase) is that the previously localised mode Φ_i can now move from site to site via virtual fluctuations into the Fermi Sea: see Fig.3, thereby providing the lattice coherence energy scale $t_0 \sim U^2/t$, below which this marginal Fermi Liquid reverts to a Fermi Liquid. Unfortunately, this means that the marginal Fermi liquid phenomenology does not persist to large U, which makes the application of our model to the cuprates rather problematic.

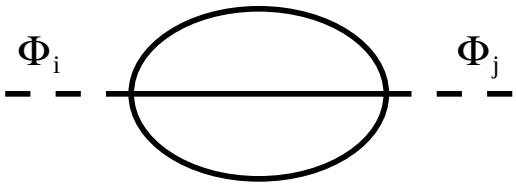

FIG. 3. Leading order diagram that generates a dispersion for the Φ_i fermion. Note that there are no arrows on the propagator lines, as all fermions are represented by Hermitian operators.

To probe the marginal fermi liquid phenomenology, we have calculated the "optical conductivity". This cannot be the ordinary electrical current, because the Hamiltonian of Eqn.15 does not conserve particle number unless $t_0 = t$ (this is most easily seen with original electron operators c, c^+). The model does have the $O(3)$ symmetry, so there is the conserved quantity $S^a = -\frac{1}{2}\sum_j \sum_{\alpha,\beta=1}^{3} \Psi_j^{(\alpha)} T^a_{\alpha\beta} \Psi_j^{(\beta)}$, where T^a are the three generators of $O(3)$. In the representation where $T^a_{\alpha\beta} = i\epsilon_{a\alpha\beta}$,

$$S^a = -\frac{i}{2}\sum_j \epsilon_{abc} \Psi_j^{(b)} \Psi_j^{(c)}. \tag{12}$$

This leads to the conserved (Noether) current:

$$j^a_{i+\hat{x}} = it\epsilon_{abc} \Psi^{(b)}_{i+\hat{x}} \Psi^{(c)}_i. \tag{13}$$

(See Methods for its derivation.) One can then define a "conductivity" which is the linear response of this $O(3)$ current to an applied field. We shall show that this $O(3)$ conductivity has the classic marginal Fermi liquid behaviour.

Within the marginal Fermi liquid regime, the $\Psi^{(a)}$ retains its marginal self-energy. The Φ mode, while having no self-energy corrections at $T = 0$ and $\omega = 0$, acquires a Fermi liquid on-site self-energy because of the virtual fluctuations into the three $\Psi^{(a)}$ (with the same diagram as Fig.3, except that site i is the same as site j). In this regime then, our model has 2 distinct quasiparticle relaxation times:

$$\Gamma_\Phi = -Im\Sigma_\Phi(\omega) \propto \omega^2 + \pi^2 T^2 \tag{14}$$

$$\Gamma_\Psi = -Im\Sigma_\Psi(\omega) \propto max[\mid \omega \mid, T] \tag{15}$$

This suggests an intriguing link to the two relaxation time phenomenology observed in the electrical and Hall conductivities of the cuprates[13], where electrical conductivity is dominated by the slower relaxation rate, while the Hall conductivity is proportional to the *product* of the two relaxation times. Unfortunately, in our model, the conserved current j^a does not include the Φ fermion, thus transport quantities constructed from this $O(3)$ current do not reveal the slow, quadratic relaxation. But another conserved quantity in our model is the total energy. Following the same strategy as for the $O(3)$ current, it can be shown that the conserved thermal current is just a sum of currents due to each of the Φ and $\Psi^{(a)}$. Now the propagators are diagonal in the Φ or Ψ operators, thus the thermal conductivity proportional to the thermal current-current correlator will just be a sum of the relaxation times: $\kappa/T \propto \frac{3t^2}{\Gamma_\Psi} + \frac{t_0^2}{\Gamma_\Phi}$. Also, any mixed correlators $\langle j^a Q^0 \rangle$ will be identically zero, where Q^0 is the thermal current due to Φ. In summary, it is unfortunately impossible to see the two relaxation times entering *multiplicatively* in any transport quantities of our model: the various conductivities derived from the $O(3)$ current will only depend on $\Psi^{(a)}$, whereas the thermal conductivity will be dominated by the largest relaxation time: that of the Φ fermion.

All of our previous considerations assume that the system does not develop into a broken symmetry state at low temperatures. In fact, as our Hamiltonian is a generalisation of the Hubbard model at half-filling, it is perhaps not surprising that it displays similar magnetic or charge ordering instabilities, due to Fermi surface nesting. The main qualitative difference is the presence of a large marginal Fermi Liquid regime in the $T - U$ phase diagram.

The plan of the paper is as follows: in Section III, we set out the formalism of Dynamical Mean Field Theory for solving the lattice model in the weak coupling regime. Section IV presents the results and Section V discusses the lattice coherence scale, and the relationship to the two-channel Kondo lattice. We also discuss the low temperature phase of the lattice when the Fermi surface has strong nesting instability. Finally, we touch on the difficulties this model faces in modelling the cuprates.

III. METHOD

We study the Hamiltonian:

$$H = i\tilde{t_0}\sum_{j,c}\Phi_{j+c}\Phi_j + i\tilde{t}\sum_{j,c}\sum_{a=1}^{3}\Psi^{(a)}_{j+c}\Psi^{(a)}_j$$
$$-U\sum_j \Phi_j\Psi^{(1)}_j\Psi^{(2)}_j\Psi^{(3)}_j. \quad (16)$$

where each fermion is a canonical Majorana fermion: $\{\Psi^{(a)}_i, \Psi^{(b)}_j\} = \delta_{ab}\delta_{ij}$, $\{\Phi_i, \Phi_j\} = \delta_{ij}$, and $\{\Psi^{(a)}_i, \Phi_j\} = 0$.

To gain some insight into the properties of the model in the weak coupling limit, we use dynamical mean field theory (DMFT)[18], a method suited to systems where the dominant interaction is on-site and spatial fluctuations are unimportant, and when the on-site temporal fluctuations at all energy scales are to be taken into account. The $d \to \infty$ limit (where DMFT is exact), requires the usual scaling $\tilde{t}_a = t_a/\sqrt{d}$, with $t_a, U \sim O(d^0)$. For a lattice of localised bound states Φ_j, $\tilde{t}_0 = 0$.

The crucial simplification in DMFT is that the self energies are k-independent as any intersite diagram (such as in Fig.3) is at most of order $1/\sqrt{d}$ relative to on-site diagrams. Now the diagram of Fig.3 is precisely that which causes the Φ fermion to propagate: omitting it means that t_0 remains at zero, and Φ_i stays localised, strictly in infinite spatial dimension. In finite d, we will need to incorporate its effect, since propagating Φ_i fields will lead to the destruction of the marginal scattering mechanism. A rigorous $1/d$ expansion appears to be formidable. Nevertheless, the essential effects of finite dimensions may be included by introducing a finite value for $\tilde{t}_0$, and treat it as a fixed parameter of the model. Defining $\tilde{t}_0 = t_0/\sqrt{d}$, we estimate t_0 by calculating the diagram (Fig.3) in finite d at $T = 0$. In Appendix A, we show that $t_0/t = c(U/t)^2/d$, with $t_a = t$ for $a = 1, 2, 3$, and c is a small constant. Finally, define a zeroth component $\Psi^{(0)}_j \equiv \Phi_j$ to get:

$$H = i\sum_{j,c}\sum_{a=0}^{3}\frac{t_a}{\sqrt{d}}\Psi^{(a)}_{j+c}\Psi^{(a)}_j - U\sum_j \Psi^{(0)}_j\Psi^{(1)}_j\Psi^{(2)}_j\Psi^{(3)}_j,$$
$$t_a = \begin{cases} t & : \quad a = 1, 2, 3 \\ t_0 & : \quad a = 0. \end{cases} \quad (17)$$

We shall use both Φ_j and $\Psi^{(0)}_j$ interchangeably.

Following standard procedures of DMFT[18], we map the lattice problem to an effective *single-site* problem with the effective action:

$$S_{eff} = \int_0^\beta d\tau d\tau' \{\sum_{a=0}^{3}\Psi^{(a)}(\tau)\mathcal{G}_a^{-1}(\tau - \tau')\Psi^{(a)}(\tau')$$
$$-U\int_0^\beta d\tau(\Psi^{(0)}\Psi^{(1)}\Psi^{(2)}\Psi^{(3)})(\tau), \quad (18)$$

where $\mathcal{G}_a(\tau)$ is the dynamical mean field at the single site which includes time dependent influence of the rest of the lattice, and is *not* the original lattice non-interacting local Green's function. It plays the role analogous to the Weiss mean field for conventional mean field theory, and has to be determined self-consistently: see below.

The effective single-site problem dressed Green's function G is related to $\mathcal{G}$ via:

$$\Sigma_a(i\omega_n) = \mathcal{G}_a^{-1}(i\omega_n) - G_a^{-1}(i\omega_n), \quad a = 0, 1, 2, 3, \quad (19)$$

where the self-energies Σ_a are calculated from S_{eff}. To lowest order in U, they are given by the following diagrams in Fig.4.

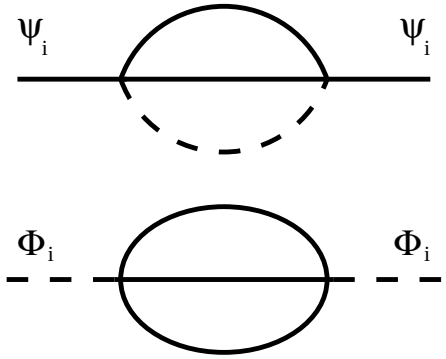

FIG. 4. On-site self-energies.

The effective single site dressed Green's function must then be related back to the $k-$average of the original lattice dressed Green's function $G_a(k, i\omega)$, via the mean field self-consistency equations[18]:

$$G_a(i\omega_n) = \int \frac{d^dk}{(2\pi)^d}G_a(k, i\omega_n),$$

where since in $d \to \infty$ limit, self-energies have no $k-$dependence, $G_a(k, i\omega_n) = 1/(i\omega_n - \epsilon_a(k) - \Sigma_a(i\omega_n))$. Doing the integration then gives[18]:

$$\mathcal{G}_a^{-1}(i\omega_n) = i\omega_n + it_a sgn(\omega_n), \quad a = 0, 1, 2, 3 \quad (20)$$

for the Lorentzian density of state (DOS): $D_a(\epsilon) = t_a/(\pi(\epsilon^2 + t_a^2))$ (corresponding to infinite range hopping); or alternatively:

$$\mathcal{G}_a^{-1}(i\omega_n) = i\omega_n - t_a^2 G_a(i\omega_n), \quad a = 0, 1, 2, 3 \quad (21)$$

for the semi-circular DOS $D_a(\epsilon) = \frac{1}{\pi t_a}\sqrt{1 - (\epsilon/2t_a)^2}$ (corresponding to nearest-neighbour hopping on a Bethe lattice). Equations 17-19 and 20 or 21, and Fig.4 together define our DMFT. The Lorentzian DOS is tractable analytically as the self-consistency equations are decoupled from G; however this also means that the effect of the lattice enters rather trivially as just a renormalisation of the bandwidth. To check these results we also use the

semi-circular DOS where the self-consistency equations are solved computationally using iterated perturbation theory[19].

One quantity of particular interest in the context of the marginal Fermi liquid is the optical conductivity. As mentioned in Section II, the Hamiltonian of Eqn.17 does not conserve particle number unless $t_0 = t$, thus the ordinary electrical current proportional to the particle current is not useful. We can however generalise the concept of the optical conductivity to this model, using the fact that the total isospin[20] $S^a = \sum_i \frac{-1}{2}\Psi_i^{(\alpha)} T^a_{\alpha\beta} \Psi_i^{(\beta)}$ is conserved, where $T^a_{\alpha\beta} = i\epsilon_{a\alpha\beta}$ are the $O(3)$ generators. Combining the continuity equation: $i\partial_\tau S_i^b + \sum_{\hat{a}} (j^b_{i+\hat{a}} - j^b_i) = 0$ ($\hat{a}$ are the unit lattice vectors), and the equation of motion $\partial_\tau S_i^b = [H, S_i^b]$ leads to the conserved current:

$$j^b_{i+\hat{x}} = it\epsilon_{b\alpha\beta}\Psi^{(\alpha)}_{i+\hat{x}}\Psi^{(\beta)}_i. \tag{22}$$

This is the Noether current associated with the $O(3)$ symmetry of our Hamiltonian. We can then introduce a vector potential field $\vec{A}^{(a)}(\vec{x}) = (A_1^{(a)} A_2^{(a)} \cdots A_d^{(a)})$ in d dimensional space, coupled to the electrons as follows:

$$H_A = it \sum_{i,c} \Psi^{(\alpha)}_{i+c} \exp\left\{ i \int d\vec{l} \cdot \vec{A}^{(a)} T^a \right\}_{\alpha\beta} \Psi^{(\beta)}_i, \tag{23}$$

where the line integral goes from site i to $i + c$, and a summation is implied over dummy indices. Since there is isotropy for $a = 1, 2, 3$, we need only study the response to the the $\vec{A}^{(1)}$ component $j_x^{(1)}(\omega) = \sum_y \sigma_{xy}(\omega) A_y^{(1)}(\omega)$, which can be described by a Kubo formula[21]:

$$\sigma_{xx}(i\omega_n) = \left. \frac{1}{-\omega_n} \Pi(\vec{q}, i\omega_n) \right|_{\vec{q}=0},$$
$$\Pi(\vec{q}, i\omega_n) = -\int_0^\beta d\tau e^{i\omega_n \tau} \langle T_\tau j_x^\dagger(\vec{q}, \tau) j_x(\vec{q}, 0) \rangle.$$

In the $d \to \infty$ limit, the absence of vertex corrections to the conductivity bubble[18] permits us to write:

$$\sigma(\nu_m) = \sum_{\vec{k}} T \sum_{\omega_n} (v_{k_x})^2 G_a(k, i\omega_n + i\nu_m) G_a(k, i\omega_n).$$

As usual, at temperatures much lower than the bandwidth, doing the Matsubara sum leads to a function peaking largely near k_F, and we replace $\sum_{\vec{k}} (v_{k_x})^2$ by $n/m \int d\epsilon$. Doing the energy integral and analytically continuing to real frequencies:

$$\sigma(\nu + i\delta) = \frac{n}{m} \int_{-\infty}^{+\infty} d\omega \left[\frac{f(\omega_-) - f(\omega_+)}{-i\nu} \right]$$
$$\times \left[\nu - (\Sigma_R(\omega_+) - \Sigma_R(\omega_-)) + i(\Gamma(\omega_+) + \Gamma(\omega_-)) \right]^{-1} \tag{24}$$

where $\Sigma(\omega \pm i0^+) = \Sigma_R(\omega) \mp i\Gamma(\omega)$ and $\omega_\pm = \omega \pm \nu/2$.

IV. RESULTS

In the $d \to \infty$ limit (ie. $t_0 = 0$), $\mathcal{G}_0$ is the same as the single impurity model, by Eqn 19 or 20, so the bound-states described by $\Psi_i^{(0)}$ are localised, with a self-energy that has a Fermi liquid form:

$$\Sigma_\Phi(\omega^+) = -(UN_0)^2 \left\{ \frac{4\omega}{\pi} + i\frac{\pi N_0}{2}(\omega^2 + (\pi T)^2) \right\}, \tag{25}$$

where $\omega^+ = \omega + i0^+$ and N_0 is the DOS at the Fermi surface. We give a brief derivation of this result in Appendix B. For $\Psi_i^{(a)}, a = 1, 2, 3$, the mean field $\mathcal{G}_a$ of the effective single site problem is of the same form as the single impurity model bare Green's function, using the Lorentzian DOS for the $d \to \infty$ lattice. This is due to the DOS in the effective problem being smooth at Fermi energy, and for $T \ll t$, equaling a constant N_0, just as in the single impurity model[10] We obtain the marginal self-energy:

$$\Sigma_\Psi(\omega^+) = -(UN_0)^2 \omega \left[\ln\frac{\Lambda}{T} - \Psi\left(1 - \frac{i\omega}{2\pi T}\right) + \frac{\pi T}{i\omega} \right], \tag{26}$$

where Λ is a cut-off proportional to t, Ψ is the Digamma function, $\gamma \sim 0.6$ is the Euler constant (Appendix B). This has the following limiting behavior

$$\Sigma_\Psi(\omega^+) = (UN_0)^2 \times \begin{cases} (-\omega \ln\frac{2\pi\Lambda}{|\omega|} - i\frac{\pi}{2}|\omega|), & (\omega \gg T) \\ (-\omega \ln\frac{\Lambda e^\gamma}{T} - i\pi T), & (\omega \ll T) \end{cases} \tag{27}$$

At finite d, the lattice coherence energy scale t_0 generated from the diagram of Fig.3 becomes finite, with $t_0 \sim U^2/t$. Marginal Fermi liquid behaviour will now persist so long as $t_0 < T \ll t$. At lower temperatures $T \ll t_0 < t$ the three-body bound-states begin to propagate coherently, causing a cross-over to Fermi liquid behavior. This is borne out by analytical calculations; here we illustrate with computational results (using the semi-circular DOS) in Fig.5 showing the effective quasiparticle scattering rate $\Gamma(\omega) = \omega Re\sigma(\omega)/Im\sigma(\omega) \sim -Im\Sigma_a(\omega^+)$, where $\sigma(\omega)$ is the optical conductivity defined in Methods. In Fig.6 we plot the the resistivity $\rho(T)$ showing the large linear T regime at weak coupling, and the inset shows the crossover to the T^2 Fermi Liquid regime.

V. DISCUSSION AND CONCLUSION

In this paper we have shown how a lattice of three-body bound-states induces marginal Fermi liquid behavior above a lattice coherence temperature t_o where a Fermi liquid forms. Since $t_0 \sim U^2/t$, a substantial window in temperature for marginal Fermi Liquid behaviour exists only for small U. The emergence of this lattice coherence energy is expected to be quite general: whenever

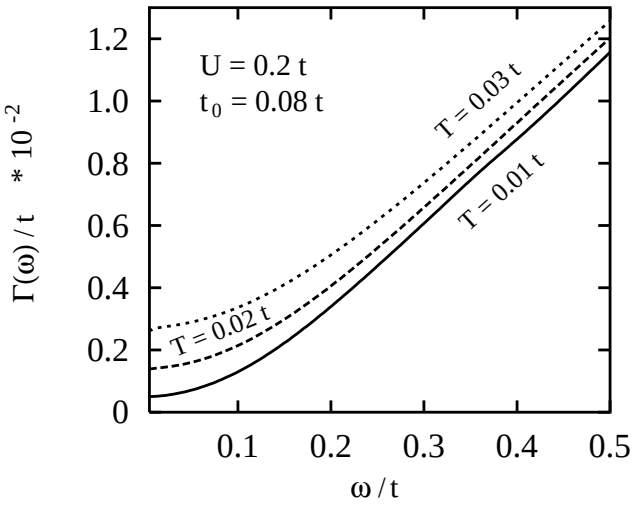

FIG. 5. Plot of quasi-particle scattering rate $\Gamma(\omega) = \omega Re\sigma / Im\sigma$.

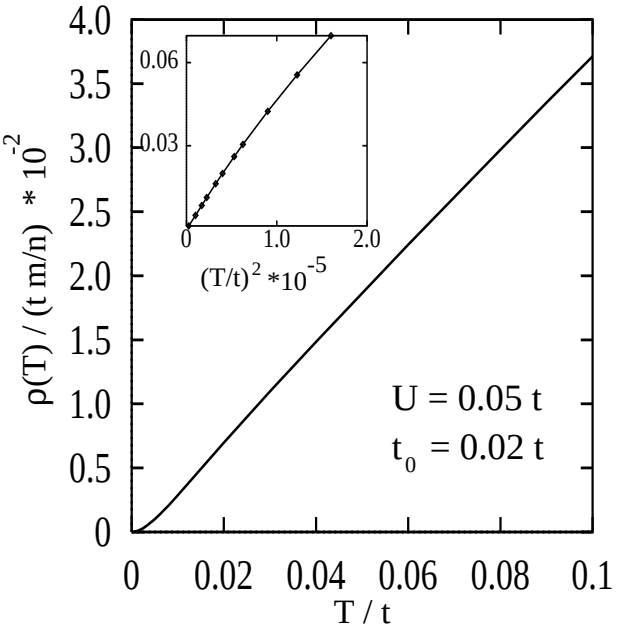

FIG. 6. Plot of resistivity vs.T. Inset shows the very low temperature crossover to T^2 behaviour: the y-axis is in the same units as the big plot.

a localised mode is allowed to interact with conduction electrons, it will be difficult to prevent hybridizations between fields at different sites. These effects however, are missed in a strict $d \to \infty$ calculation.

This brings us onto the question of the relationship between our lattice model and the two-channel Kondo lattice model. The single-impurity version of the Hamiltonian of Eqn.11 (with $U < 0$) was originally derived[10] in the context of the single-impurity two-channel Kondo model[24]. That derivation took advantage of spin-charge separation[16] to throw away uncoupled (charge) degrees of freedom, and it has been shown via bosonization to be exactly equivalent to the original model[17]. Unfortunately there is no such relation between the two-channel Kondo lattice and the Majorana lattice considered here.

In the above calculations, we have assumed that the marginal Fermi Liquid state is unstable only to the Fermi Liquid state at low T. In fact, just as in the Hubbard model , a mean field calculation indicates that for a Fermi surface with a strong nesting instability (for example, nearest neighbour hopping in a hypercubic lattice), there is a phase transition to antiferromagnetic order (for $U > 0$). The order parameter is a vector that reflects the $O(3)$ symmetry of the model:

$$V^a(\vec{x}_j) = e^{iQ\cdot x_j}\langle c^\dagger_\alpha \sigma^a_{\alpha\beta} c_\beta\rangle = ie^{iQ\cdot x_j}\left\langle \Psi^{(0)}\Psi^{(a)} - \frac{1}{2}\left(\vec{\Psi}\times\vec{\Psi}\right)^a\right\rangle, \qquad (28)$$

where $Q = (\pi, \ldots, \pi)$ is the nesting vector. From the divergence in the susceptibility, we find that at weak coupling, $T_c < t_0$, except when $t_0 = 0$:

$$\frac{T_c}{\Lambda} = \exp\left[\frac{\ln t_0/t}{4} - \sqrt{\frac{(\ln t_0/t)^2}{4} + \frac{1+t_0/t}{2(UN_0)^2}}\right], \qquad (29)$$

where Λ is a cut-off ($\Lambda < t$). (Note that this reduces to the Hubbard model value when $t_0 = t$.) At $t_0 = 0$, T_c is identical to the Hubbard case. For $0 < t_0 < t$, T_c is enhanced relative to the Hubbard case. Hence a region of Fermi liquid phase separates the low temperature antiferromagnetic phase from the marginal Fermi Liquid regime: Fig.7.

There are further similarities to the Hubbard model at half-filling. Both of the $SO(4)$ and $O(3)$ models are invariant under $U \to -U$ and $\Psi^{(0)} \to -\Psi^{(0)}$. The latter map corresponds to a particle-hole transformation for the down spin only: $c_\downarrow \leftrightarrow c^+_\downarrow$. This implies that in going from the positive U model to the negative U model, magnetic ordering turns into charge ordering[25] . It can also be shown that neither model mixes charge and magnetic ordering. Further, both models reduce to the Heisenberg antiferromagnet as $U \to \infty$. Thus our model has very similar properties to the half-filled Hubbard model, except for the marginal Fermi Liquid phase at weak coupling.

What insight does our model bring towards the understanding of the marginal Fermi liquid behaviour in the

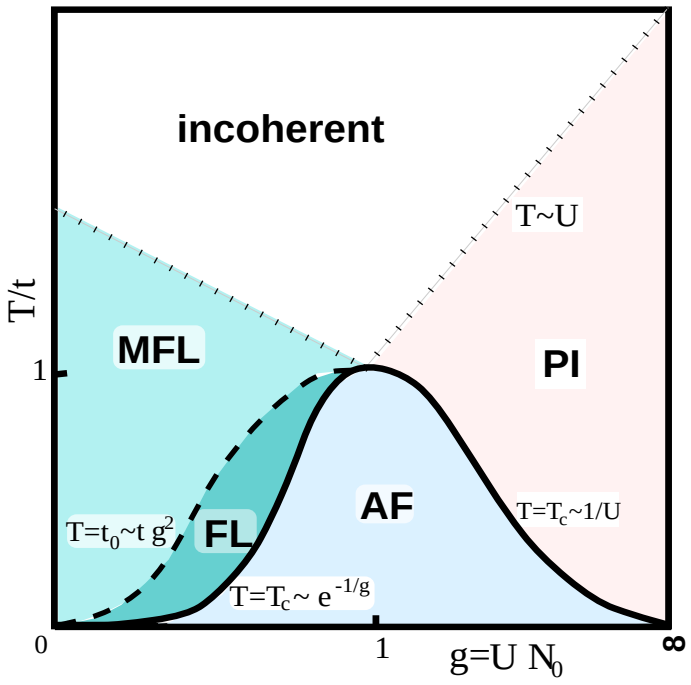

FIG. 7. Schematic phase diagram of the Majorana lattice model. The dimensionless coupling is $g \equiv UN_0$ where $N_0 \propto 1/t$ is the density of states at the Fermi surface. $t_0 = ctg^2/d$. MFL is the marginal Fermi liquid phase, FL is the Fermi liquid phase. AF is the antiferromagnetic phase, PI is the paramagnetic insulating phase. At weak coupling, T_c goes as $\exp(-1/g)$, while at strong coupling, it goes as t^2/U. We have no computation for strong coupling for $T > T_c$, thus we do not know the continuation of the $T = t_0$ line. However, we might expect that when U is of order t, T_c and t_0 will also be of order t. One scenario is then the $T = t_0$ line meets and ends at the $T = T_c$ line around t_0. Also, at strong coupling, the paramagnetic insulator crosses over to a metal at $T \sim U$ (in analogy to the Hubbard model), and in the weak coupling regime, there will be a similar high temperature cross-over from marginal Fermi Liquid to an incoherent metallic phase: these cross-overs are indicated with a dotted line.

cuprates? While our model does provide a simple lattice realisation of a marginal Fermi liquid, it unfortunately suffers from a number of defects:

- It has a wide window of marginal Fermi liquid behaviour only for small coupling. The cuprates are believed to be in the strong coupling regime[22], but at strong coupling, our system has charge or magnetic instabilities. Related to this is the fact that in the cuprates, the inelastic scattering rate $\Gamma = \Gamma_0 \max[\omega, T]$ has Γ_0/t a constant of order one, whereas our model has Γ_0/t proportional to the coupling squared.

- The model needs to be at half filling: upon doping, a chemical potential term $\mu(\Psi^{(0)}\Psi^{(3)} + \Psi^{(1)}\Psi^{(2)})$ leads to a width $\Delta \propto \mu^2$ for Φ, with Fermi liquid properties when $T < \Delta$. This seems to require fine tuning, contradicting the rather robust linear-T resistivity observed even in underdoped systems (above the "spin gap" scale).

- Despite the presence of two relaxation rates in the system, transport quantities will not involve a multiplicative combination of the Φ and Ψ relaxation rates, as is postulated in the two-relaxation-times phenomenology for the cuprates. (See Section II.)

In conclusion we have demonstrated the persistence of marginal Fermi Liquid behaviour at weak coupling in a toy model of a marginal Fermi Liquid in an infinite dimensional lattice. For finite d, the lattice coherence energy cuts off marginal Fermi Liquid behaviour and the system reverts to a Fermi Liquid at low temperatures. Since this cut-off grows with the coupling, there will be no marginal Fermi Liquid regime at strong coupling. It remains to be seen if a strong coupling marginal Fermi Liquid exists in any finite dimensions.

Acknowledgement We acknowledge useful discussions with Andrew Schofield, Gunnar Pálsson and Revaz Ramazashvili. This work was supported by NSF grant DMR-96-14999. Part of the work was done while the authors were in the Non-Fermi Liquid Workshop at the Institute of Theoretical Physics (ITP), UCSB, funded under NSF grant PHYS94-07194 and DMR-92-23217. We thank the staff at ITP for their hospitality.

VI. APPENDIX A: CALCULATION OF THE EFFECTIVE BANDWIDTH t_0

We want to estimate in finite dimensions the effective kinetic energy $i\tilde{t}_0 \sum_{i,c} \Psi^{(0)}_{i+c}\Psi^{(0)}_i$ from the zero-frequency part of the $\Psi^{(0)}$ self-energy, as depicted in Fig.3, to lowest order in the coupling:

$$i\tilde{t}_0 = U^2 \int_0^\beta d\tau [G_{\hat{x}}(\tau)]^3 \tag{30}$$

where $G_{\hat{x}}(\tau)$ is the bare propagator of $\Psi^{(a)}(a=1,2,3)$, for nearest neighbour sites, taken here to be in the $\hat{x}$ direction. In k,ω space, $G(\vec{k},i\omega_n)=[i\omega_n-\epsilon_{\vec{k}}]^{-1}$. For simplicity, take $\epsilon_{\vec{k}}=-2\tilde{t}\sum_{i=1}^{d}\sin(k_i)$, appropriate for the hypercubic nearest neighbour dispersion. (We expect that as $T\to 0$, the exact shape for the band does not matter.) Let $\tilde{t}=t/\sqrt{d}$ and $\tilde{t}_0=t_0/\sqrt{d}$, as required for a proper scaling of the kinetic energy term in large d limit. Then $G_{\hat{x}}(\tau)$ will be of order $1/\sqrt{d}$, and as mentioned in the Methods section, $\tilde{t}_0\sim O(d^{-3/2})$, ie., $1/d$ down on the dispersion for the $a=1,2,3$ components. Doing the standard Matsubara sum leads to:

$$G_{\hat{x}}(\tau)=\int\frac{d^dk}{(2\pi)^d}f(-\epsilon_{\vec{k}})\exp(i\vec{k}\cdot\hat{x}-\epsilon_{\vec{k}}\tau). \tag{31}$$

In the zero temperature limit, the Fermi function become $f(-\epsilon_{\vec{k}})\to\theta(\epsilon_{k_x}+\epsilon'_{\vec{k}})$, where we have split up the dispersion into the k_x part and the other $d-1$ part. Turning the $d-1$ dimensional $k-$integral into an energy integral gives:

$$G_{\hat{x}}(\tau)=\int\frac{dk_x}{(2\pi)}e^{ik_x-\epsilon_{k_x}\tau}\int_{-\epsilon_{k_x}}^{\infty}d\epsilon N(\epsilon)e^{-\epsilon\tau}, \tag{32}$$

where $N(\epsilon)$ is the density of states in $d-1$ dimensions.

To make further progress, a flat density of states is used: $N(\epsilon)=1/(4t)$ for $|\epsilon|<2t$ and zero otherwise. Thus, defining the dimensionless time variable $s=2\tau t$,

$$G_{\hat{x}}(s)=-\frac{e^{-s}}{2s}J_1(i\frac{s}{\sqrt{d}}), \tag{33}$$

where $J_1(z)=\int_{-\pi}^{\pi}\frac{dx}{2\pi}e^{-iz\sin(x)+ix}$ is the Bessel function of the first kind of the first order. Thanks to the factor of $1/\sqrt{d}$ inside its argument, the Bessel function asymptotically always grows more slowly than the decay due to the e^{-s} factor. (For $|arg(z)|<\pi$ and $|z|\to\infty$, $J_1(z)\to(\frac{2}{\pi z})^{1/2}\cos(z-3\pi/4)$.) Thus, contributions to the integral in Eqn.30 are dominated by the regime when the Bessel function is at most of order one, allowing us to approximate: $iJ_1(ix)=-x/2+O(x^3)$ in Eqn.33, leading finally to:

$$\begin{aligned}\tilde{t}_0&\simeq\frac{U^2}{2t}\int_0^{\infty}ds\left[\frac{e^{-s}}{2s}\frac{s}{2\sqrt{d}}\right]^3\\&=\frac{U^2}{2^7\cdot 3\quad t\quad d^{3/2}},\end{aligned} \tag{34}$$

with $\tilde{t}_0$ of order $d^{-3/2}$ as claimed.

VII. APPENDIX B: CALCULATION OF THE MARGINAL SELF-ENERGY

To order U^2, the on-site self-energy for $\Psi_i^{(a)}$, $a=1,2,3$ is:

$$\Sigma_\Psi(\tau)=U^2\mathcal{G}_0(\tau)\mathcal{G}_a(\tau)\mathcal{G}_a(\tau). \tag{35}$$

$\mathcal{G}_0(\tau)=sgn(\tau)/2$ is identical to the single impurity $\Psi^{(0)}$ propagator[10], since in the strict $d\to\infty$ limit, $t_0=0$. For $\Psi_i^{(a)}$,

$$\mathcal{G}_a(\tau)=T\sum_{\omega_n}\frac{e^{-i\omega_n\tau}}{i\omega_n+it_a sgn(\omega_n)} \tag{36}$$

where we have used Eqn.19 for $\mathcal{G}_a(i\omega_n)$ for the Lorentzian DOS. As usual, turn the Matusbara sum into a contour integral and deform the contour onto the branch cut at the real axis to get:

$$\mathcal{G}_a(\tau)=-Im\int_{-\infty}^{\infty}\frac{d\omega}{\pi}(1-f(\omega))\frac{e^{-\omega\tau}}{\omega+it_a}. \tag{37}$$

($f(\omega)$ is the Fermi function.) As we are interested in $T\ll t_a$, the integrand is dominated by small ω, and we approximate the denominator $\omega+it_a\approx it_a$. Now the $d-$dimensional Lorentzian DOS at the Fermi surface is $N_0=1/(\pi t_a)$, and thus $\mathcal{G}_a(\tau)$ is identical to that for the single impurity calculation[10]:

$$\mathcal{G}_a(\tau)=\frac{N_0\pi T}{\sin(\tau\pi T)}. \tag{38}$$

Note that this expression is accurate for $0\ll\tau\ll\beta$. Going to Matsubara frequencies $\omega_n=(2n+1)\pi T$:

$$\begin{aligned}\Sigma_\Psi(i\omega_n)&=U^2\int_0^{\beta}d\tau\frac{sgn(\tau)}{2}\left(\frac{N_0\pi T}{\sin(\tau\pi T)}\right)^2e^{-i\omega_n\tau}\\&=-i\frac{\pi T}{2}(UN_0)^2I_n(\epsilon)\end{aligned} \tag{39}$$

where

$$I_n(\epsilon)=\int_{\epsilon}^{\pi-\epsilon}dx\frac{\sin(2n+1)}{(\sin(x))^2}. \tag{40}$$

We have put in a cut off $\epsilon=\pi T/(2t_a)\ll 1$. Integrating by parts twice, and using the tabulated integral[26]: $\int_0^{\pi}dx\ln\sin(x)\sin(2n+1)x=-\frac{2}{2n+1}(\frac{1}{2n+1}+\ln 2+\gamma+\Psi(n+1/2))$, we get:

$$I_n(\epsilon)=\frac{2\omega_n}{\pi T}\left(\ln\left(\frac{\Lambda}{T}\right)-\Psi\left(\frac{\omega_n}{2\pi T}\right)\right)-2. \tag{41}$$

$\Psi(x)$ is the Digamma function, $\Lambda=t_ae^{1-\gamma}/(\pi T)$ and $\gamma\sim 0.6$ is the Euler constant. (We have expanded in ϵ and kept only the terms up to ϵ^0.) Putting this all together and performing the analytic continuation $i\omega_n\to\omega+i0^+$ gives Eqn. 26.

The on-site self-energy for Φ is:

$$\Sigma_\Phi(\tau)=U^2\mathcal{G}_a(\tau)\mathcal{G}_a(\tau)\mathcal{G}_a(\tau). \tag{42}$$

Fourier transforming:

$$\Sigma_\Phi(i\omega_n) = iN_0(N_0U\pi T)^2 K_n, \qquad (43)$$
$$K_n = \int_\epsilon^{\pi-\epsilon} dx \frac{\sin(2n+1)x}{(\sin(x))^3}.$$

Again, we have a cut-off $\epsilon = \pi T/(2t_a) \ll 1$. Integrating by parts and expanding in ϵ, $K_n = 2(2n+1)/\epsilon - 2n(n+1)\pi$. This then leads to Eqn. 25 after analytic continuation.

---

[1] C. M. Varma, P. B. Littlewood, S. Schmitt-Rink, E. Abrahams and A. E. Ruckenstein, Phys. Rev. Lett. **63**, 1996, (1989).

[2] Z. Schlesinger et. al. Phys. Rev. Lett. **65**, 801, (1990).

[3] A. El Azruk, R. Nahoum, N. Bontemps, M. Guilloux-Viry, C. Thivet, A. Perrin, S. Labdi, Z. Z. Li and H. Raffy, Phys. Rev. **B 49**, 9846, (1994).

[4] A. V. Puchkov, D. N. Basov and T. Timusk, J. Phys. Condens. Mat. **48**, 10049, (1996).

[5] J. E. Hirsch and D. J. Scalapino, Phys. Rev. Lett. **56**, 2732 (1986), D. M. Newns et. al. Phys. Rev. Lett **73**, 1695 (1994). For further references, see the review R. S. Markiewicz, cond-mat/9611238.

[6] L. B. Ioffe and A. I. Larkin, Phys. Rev. **B 39**, 8988 (1989), G. Kotliar, Phys. Rev. **B 37**, 3664 (1989), P. A. Lee and N. Nagaosa, Phys. Rev. **B 46**,5621 (1992).

[7] A. Sokol and D. Pines, Phys. Rev. Lett. **71**, 2813. (1993)

[8] For the most recent and comprehensive review of Anderson's thinking,see P. W. Anderson "The Theory of Superconductivity in the High T_c Cuprates", Princeton University Press, Princeton, NJ. (1997)

[9] A. E. Ruckenstein and C. M. Varma, Physica **C 185-189**, 134, (1991).

[10] P. Coleman, L. Ioffe and A. M. Tsvelik, Phys. Rev. **B52**, 6611 (1995).

[11] I. Affleck, Lecture at the NATO Advanced Study Institute on *Physics, Geometry and Topology*, Banff (1989)

[12] C. N. Yang and S. C. Zhang, Mod. Phys. Lett. **B4**, 759, (1990).

[13] P. W. Anderson, Phys. Rev. Lett. **67**, 2092 (1991), P. Coleman, A. J. Schofield, and A. M. Tsvelik, J. Phys. (Cond. Matt.) **8**, 9985 (1996).

[14] E. Majorana, Il Nuovo Cimento, **14**, 171 (1937).

[15] P. Coleman, E. Miranda and A. M. Tsvelik, Phys. Rev. Lett. **74**, 1653 (1995).

[16] V. J. Emery and S. Kivelson, Phys. Rev. **B46**, 10812 (1992),

[17] A. J. Schofield, cond-mat/9606063 (1996). G.-M. Zhang, A. C. Hewson and R. Bulla cond-mat/9705199 (1997)

[18] See the review of A. Georges, G. Kotliar, W. Krauth and M. J. Rozenberg, Rev. Mod. Phys. **68**, 13, (1996). All other technical points about DMFT mentioned in our paper is explained in detail here.

[19] A. Georges and G. Kotliar (1992). We modify their algorithm slightly by doing the self-consistency loop with the spectral weights $\rho_a(\omega) = -\frac{1}{\pi} ImG_a(i\omega_n \to \omega + i0^+)$ rather than $G(i\omega_n)$, and the self-consistency equations become $\rho_a(\omega) = \frac{1}{\pi t_a}\{Im\Sigma(\omega+i0^+)/t + Im\sqrt{(\frac{\omega-\Sigma(\omega+i0^+)}{t_a})^2 - 2}\}$.

[20] This is the Majorana ($O(3)$) representation of a spin$-1/2$ operator, see eg. D.C. Mattis, "The Theory of Magnetism I", Springer Verlag (1988), and A. M. Tsvelik, "Quantum Field Theory in Condensed Matter Physics", Cambridge University Press, (1995).

[21] See eg. G. D. Mahan, "Many Particle Physics", Plenum, (1991).

[22] See eg. M. S. Hybertsen, M. Schlüter, and N. E. Christensen, Phys. Rev. **B39**, 9028, (1989). They estimated U on copper sites to be around 10.5 eV, versus oxygen-copper hopping $\sim 1.3eV$.

[23] M. Jarell, H. Pang, D. L. Cox, F. Anders, and A. Chattopadhyay preprint cond-mat/9609146 (1996), D. L. Cox and M. Jarell, J. Phs. Condens. Matter **8**, 9825, (1996). It should be noted that our model here, although inspired by the compactified version of the single impurity two channel Kondo model, bears *no* simple relation to the two-channel Kondo lattice.

[24] P. Nozières and A. Blandin, J. Phys. (Paris) **41**, 193 (1980).

[25] This is well known for the Hubbard model, see eg., E. Fradkin, "Field Theories in Condensed Matter Systems", Addison-Wesley (1991). But the derivation in terms of Majaorana fermions is new and simple.

[26] I. S. Gradshteyn and I. M. Ryzhik, "Table of Integrals, Series, and Products" 5th edition, no. 4.384.2 , Academic Press, London (1994)